Journal of Hazardous Materials 162 (2009) 133–139

Contents lists available at ScienceDirect

Journal of Hazardous Materials

journal homepage: www.elsevier.com/locate/jhazmat

Adsorption of anionic dyes on ammonium-functionalized MCM-41

Qingdong Qin, Jun Ma*, Ke Liu

School of Municipal and Environmental Engineering, Harbin Institute of Technology, P.O. Box 2627, 202 Haihe Road, Harbin 150090, PR China

ARTICLE INFO

Article history:
Received 8 January 2008
Received in revised form 7 April 2008
Accepted 5 May 2008
Available online 9 May 2008

Keywords:
Adsorption
Anionic dye
Kinetics
Ammonium-functionalized MCM-41
Isotherm

ABSTRACT

Investigations were conducted in a batch reactor system to study the adsorption behavior of four anionic dyes (Methyl orange (MO), Orange IV (OIV), Reactive brilliant red X-3B (X-3B), and Acid fuchsine (AF)) on ammonium-functionalized MCM-41 (NH_3^+-MCM-41) from aqueous medium by varying the parameters such as contact time, initial dye concentration, pH and competitive anions. Dye adsorption was broadly independent of initial dye concentration. The intraparticle diffusion model was the best in describing the adsorption kinetics for the four anionic dyes on NH_3^+-MCM-41. The adsorption data for the four dyes were well fitted with the Langmuir model. The electrostatic interaction was considered to be the main mechanism for the dye adsorption. Finally, it was observed that the anion of soft acid inhibited the adsorption capacity significantly.

© 2008 Elsevier B.V. All rights reserved.

1. Introduction

It is well known that textile industries, pulp mills and dyestuff manufacturing discharge highly colored wastewaters which have provoked serious environmental concerns all over the world [1,2]. Color is the first contaminant to be recognized in wastewater. The presence of very small amounts of dyes in water (less than 1 ppm for some dyes) is highly visible and aesthetically unpleasant. In addition, several classes of dyes are stable molecules that are resistant to degradation by light, chemical, biological and other exposures and are considered as possible carcinogens or mutagens to humans [3]. Therefore, it is necessary to reduce dye concentration in the wastewater before it is released into the marine environment.

Various treatment processes such as physical separation, chemical oxidation and biological degradation have been widely investigated to remove dyes from wastewaters. Amongst the numerous techniques of dye removal, considerable attention has been paid to adsorption technologies as efficient and versatile methods for removing dyes from wastewater effluents [3]. The removal of dyes from wastewater is considered to be an important application of adsorption process using suitable adsorbent. Highly functional porous materials with high surface areas are generally used for such applications because they show excellent removal efficiency [4]. Many micromesoporous, crystalline, and amorphous families of adsorbents, for example, zeolites, activated carbons, wood chips, ion-exchange resins, and polymeric adsorbents, with a wide spectrum of surface chemistry and pore structure, have been used to carry out the desired separations [5–7]. Nowadays, the discovery of ordered mesoporous materials has aroused a worldwide resurgence in the synthesis, characterization, and application of these materials [8].

MCM-41, one member of the mesoporous molecular sieves M41S family, possesses a high specific surface and a regular hexagonal array of cylindrical pores, which is largely used in shape-selective catalysis, selective adsorption and separation processes, chemical sensors, as well as nanotechnology [9]. Such material is characterized by large surface areas, narrow pore-size distribution and a moderate hydrophobic character. Recently, MCM-41 has been used to adsorb basic dye from wastewater and is proven to be an effective adsorbent for the removal of basic dyes [10–12]. It is well known that MCM-41 has a negative charge density due to the presence of Si-O and Si-OH groups, which should adsorb positive charged dyes and do not permit the adsorption of negative ones. In the design of improved MCM-41 for the adsorption of specific substance, surface modification is very helpful in the improvement of the adsorption capacity and selectivity of the MCM-41 by taking advantage of specific interactions between the adsorbents and the adsorbates [13,14].

In the present study, the modification of MCM-41 by 3-aminopropyltrimethoxysilane (APTS) was attempted, and the NH_3^+-MCM-41 was used to remove four types of anionic dyes, MO, OIV, X-3B and AF with different molecular configurations. The adsorption processes with respect to contact time, pH, and competitive anions were measured to provide more information about the

* Corresponding author. Tel.: +86 451 86282292; fax: +86 451 82368074.
E-mail address: majun@hit.edu.cn (J. Ma).

0304-3894/$ – see front matter © 2008 Elsevier B.V. All rights reserved.
doi:10.1016/j.jhazmat.2008.05.016

Table 1
The general data of four types of anionic dyes used in this work

Dye	Classification		Formula	Molecular volume (g mol^{-1})	λ_{max} (nm)[a]
MO	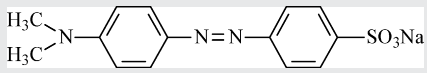	Anionic monoazo	$C_{14}H_{14}N_3O_3SNa$	327.3	464
OIV	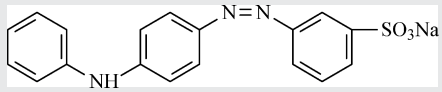	Anionic monoazo	$C_{18}H_{15}N_3O_3SNa$	375.4	476
AF	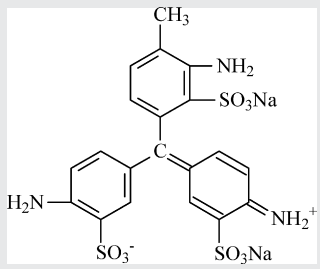	Anionic triphenylmethane	$C_{20}H_{17}N_3O_9S_3Na_2$	585.5	544
X-3B	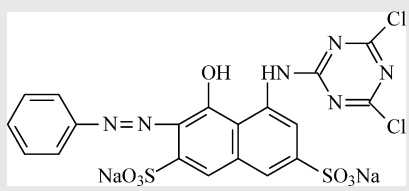	Anionic monoazo	$C_{19}H_{10}Cl_2N_6O_7S_2$ Na_2	615.3	538

[a] Determined by Unic UV–vis spectrophotometer UV-4802 over a range from 190 to 1000 nm.

adsorption characteristics of NH_3^+-MCM-41. The equilibrium data were fitted into Langmuir equation to determine the correlation between the isotherm models and the experimental data. The kinetic parameters were calculated to determine the adsorption mechanism.

2. Materials and methods

2.1. Preparation of adsorbent

The MCM-41 mesoporous silica was synthesized in classical alkaline medium using conventional literature recipes [15]. Modification of calcined MCM-41 with APTS was conducted as follows [16]. 5 mL of APTS was mixed with 4 g of MCM-41 powder in 50 mL of anhydrous toluene (for 24 h under reflux conditions and a nitrogen atmosphere). The resulting modified MCM-41 was filtered off and washed with toluene and methanol. Finally, the product was heated for 8 h at 110 °C under vacuum condition and was designated as NH_2-MCM-41. The material was then acidified using HCl solution in order to protonate the amino groups leading to positively charged ammonium moieties [13]. Therefore, 0.1 g of NH_2-MCM-41 was stirred in 100 mL of 0.1 mol L^{-1} HCl for 5 h at room temperature. The acidified material, designated as NH_3^+-MCM-41, was recovered by filtration and dried at ambient temperature overnight. The BET surface area of NH_3^+-MCM-41 was 403 m^2 g^{-1}. The average pore diameter was 2.54 nm.

2.2. Adsorbates

Four types of anionic dyes (MO, OIV, AF with 99 % purity and X-3B with 80% purity) were used to test the adsorption capacity of NH_3^+-MCM-41 without further purification. Their chemical structures and general data are shown in Table 1. The dye stock solutions were prepared by dissolving accurately weighed dyes in distilled water to the desired concentration. The experimental solutions were obtained by diluting the dye stock solutions in accurate proportions to different initial concentrations.

2.3. Adsorption experiments

Adsorption experiments were performed by batch technique to obtain the adsorption rate and equilibrium data. The dye adsorption experiments were all conducted in distilled water (pH 5.6) and room temperature. For the experiments of adsorption kinetics, a suspension containing 0.04 g of NH_3^+-MCM-41 was mixed by stirring the mixture at 200 rpm with a 200 mL aqueous solution of dye at a known initial concentration in a flask that was immersed in a temperature-controlled water bath kept at constant working temperature (24.5 ± 0.5 °C). An aliquot of the solution was withdrawn at appropriate time intervals and filtered by a glass fiber with 0.7 μm pore size. Then the residual concentration of dye in the filtrate was subsequently determined using the spectrophotometer at the wavelength corresponding to the maximum absorbance. For the adsorption isotherm experiments, a given amount of adsorbent (0.005 g) was placed in a 50-mL flask, into which 10 mL of each dye solution with varying concentrations was added. The experiments were performed in a temperature-controlled water bath shaker for the desired time periods at a mixing speed of 180 rpm. The contact time was selected on the basis of preliminary experiments, which demonstrated that the equilibrium of adsorption was established in 24 h. After this period, the solutions were filtered and analyzed for the remaining concentration of dye. The amount of dye adsorbed onto NH_3^+-MCM-41 was calculated from the mass balance equation as:

$$q_e = \frac{(C_0 - C_e)V}{M} \quad (1)$$

where q_e (mmol g^{-1}) is the amount of dye adsorbed per gram of NH_3^+-MCM-41 at equilibrium; C_0 (mmol L^{-1}) and C_e (mmol L^{-1}) are the initial and equilibrium liquid-phase concentration of dye,

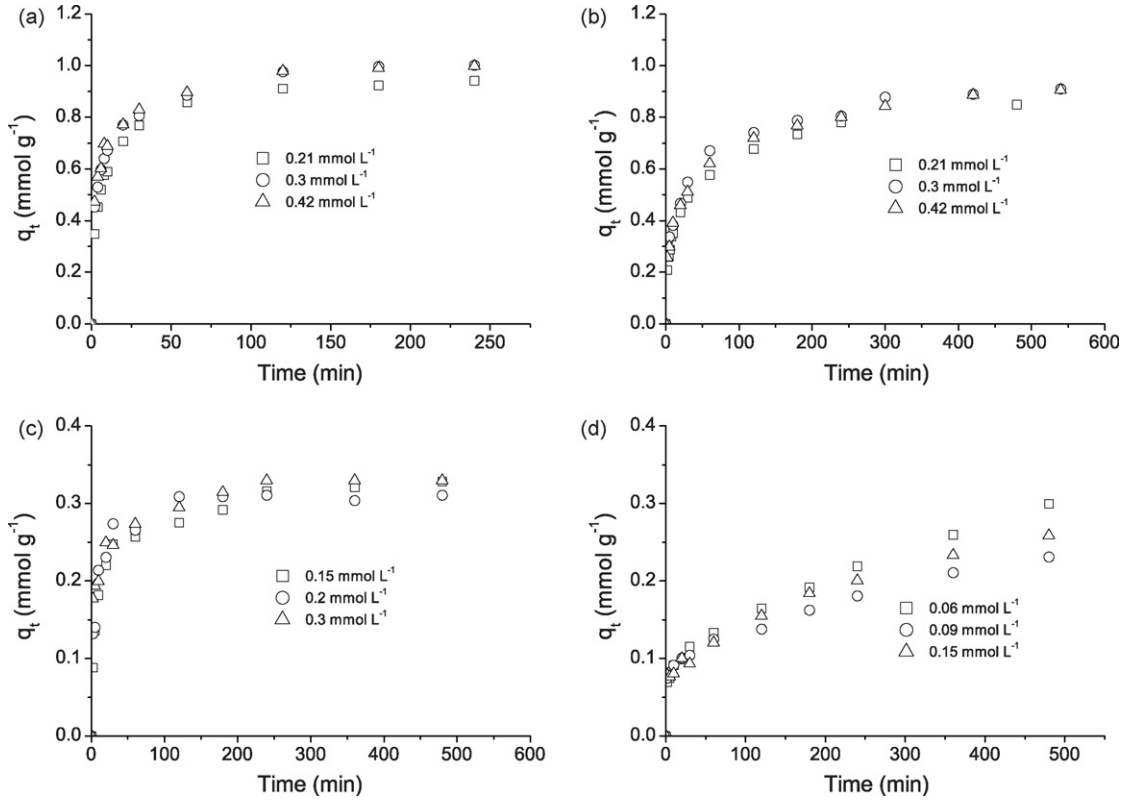

Fig. 1. Effect of initial concentration on the adsorption rate of dye with the NH_3^+-MCM-41: (a) MO; (b) OIV; (c) AF; (d) X-3B.

respectively; V (L) is the volume of dye solution and M (g) is the mass of NH_3^+-MCM-41 used.

2.4. Effect of solution pH and competitive anions on dye adsorption

The effect of solution pH on dye adsorption was investigated according to the following procedure. A mass of 0.02 g of dried NH_3^+-MCM-41 was added to a number of 25 mL glass bottles containing 10 mL of dye solution. The pH of the dye solutions was adjusted to a pH range from 4.0 to 10.0 using 0.5 mol L^{-1} HCl or 0.5 mol L^{-1} NaOH solutions (prior to the addition of the adsorbent). The bottles were then sealed and placed in the shaker at 24.5 ± 0.5 °C for 24 h. The effect of competitive anions, such as phosphate, nitrate, sulfate and carbonate, on the adsorption of the dye was investigated according to the following procedure. A mass of 0.02 g of dried NH_3^+-MCM-41 was added to a number of 25 mL glass bottles containing 10 mL of dye solution with 0.01 mol L^{-1} anion. After 24 h, the solution phase dye concentration was determined.

2.5. Zeta potential measurements

Zeta potential measurements were conducted using a Zeta-Sizer 3000 (Malvern Instrument). The sample containing 0.2 g L^{-1} NH_3^+-MCM-41 was suspended in a 0.01 mol L^{-1} NaCl solution (electrolyte) and the aqueous suspension with or without dye was equilibrated at initial pH 5.6 for 24 h. Then, the equilibrated slurry was injected into the microelectrophoresis cell using disposable syringes to determine the zeta potential at different pH values. Prior to each measurement, the electrophoresis cell was thoroughly washed and rinsed with deionized water, followed by the introduction of the sample solution to be measured.

3. Results and discussion

3.1. Kinetics of adsorption

In order to investigate the mechanism of adsorption and potential rate controlling steps, the kinetic behavior of the adsorption process was studied under the temperature of 24.5 ± 0.5 °C and pH 5.6 using different initial dye concentrations (Fig. 1). It appears from Fig. 1a that, for all concentrations of MO, there was a rapid uptake of MO during the initial stage of the adsorption process within the first 2 min, indicating a high affinity between MO molecules and the NH_3^+-MCM-41 surface. Following this phase, the adsorption process slows, suggesting a gradual equilibrium, possibly due to the intraparticle diffusion of MO molecules. Finally, the saturation is reached, showing the final equilibrium at approximately 240 min, beyond which no further adsorption takes place. The equilibrium time is independent of initial dye concentration. The adsorption capacity of MO for 4 h with initial dye concentrations of 0.21, 0.3 and 0.42 mmol L^{-1} are 0.94, 1.00 and 1.00 mmol g^{-1}, respectively. This indicates that the adsorption capacity of MO on NH_3^+-MCM-41 is independent of initial dye concentrations. The similar effect is also obtained by OIV, AF and X-3B.

Kinetic modeling not only allows estimation of adsorption rates but also leads to suitable rate expressions, characteristic of possible reaction mechanisms. In this respect, the pseudo-first-order, pseudo-second-order and intraparticle equations were used to test the experimental data of different initial concentration [17].

The first-order rate expression is given as:

$$\frac{dq_t}{dt} = k_1(q_e - q_t) \quad (2)$$

where q_e and q_t are the amounts of dye adsorbed on adsorbent at equilibrium and at time t, respectively (mmol g^{-1}), and k_1 is

the rate constant of pseudo-first-order adsorption (min^{-1}). After integration, with the initial conditions $q_t = 0$ at $t = 0$, the equation becomes:

$$q_t = q_e(1 - e^{-k_1 t}) \quad (3)$$

The pseudo-second-order kinetic model is expressed by the following equation:

$$\frac{dq_t}{dt} = k_2(q_e - q_t)^2 \quad (4)$$

where k_2 is the rate constant of the pseudo-second-order model ($g\,mmol^{-1}\ min^{-1}$). This model is based on the assumption that the rate-limiting step involves chemisorption of adsorbate on the adsorbent. The following integrated form can be obtained:

$$q_t = \frac{k_2 q_e^2 t}{1 + k_2 q_e t} \quad (5)$$

The rate parameter of intraparticle diffusion can be defined as:

$$q_t = k_{iP} t^{0.5} \quad (6)$$

where k_{iP} is the intraparticle diffusion rate constant ($mmol\,g^{-1}\,min^{0.5}$). The k_{iP} values under different conditions were calculated from the slopes of the straight line portions of the respective plots.

In order to quantitatively compare the applicability of different kinetic models in fitting to data, a normalized standard deviation, Δq (%), was calculated

$$\Delta q\,(\%) = 100 \times \sqrt{\frac{\sum [(q_{t\,exp} - q_{tcal})/q_{t\,exp}]^2}{n-1}} \quad (7)$$

where n is the number of data points; q_{texp} is the experimental values; and q_{tcal} is the calculated values by the model.

The results from fitting experimental data with pseudo-first and pseudo-second-order models and intraparticle diffusion model are presented in Table 2. It is observed that the order of Δq is pseudo-first > pseudo-second > intraparticle diffusion model for four types of anionic dyes, which indicates that the intraparticle diffusion model is the best one in describing the adsorption kinetics of anionic dyes on NH_3^+-MCM-41. The results in Table 2 also indicate that, for four types of anionic dyes, the value of k_{1P} increased as the initial dye concentration increased. Generally the driving force changes with the dye concentration in bulk solution. The increase in dye concentration results in the increase of driving force, which consequently increases the diffusion rate of the molecular dye from bulk phase to the exterior surface of adsorbent. However, the effect of the initial dye concentration on k_{2P} and k_{3P} was not significant. It is assumed that the diffusion resistance which is caused by the size of the adsorbate molecule and the pore-size distribution of the adsorbent is larger than the driving force of diffusion. Finally, the increase in the driving force of diffusion can be neglected when the dye diffuses in the pores of the particles.

In general, three consecutive mass transfer steps are associated with the adsorption of solute from solution by porous adsorbent, any of which could be the rate-controlling factor. First, the adsorbate migrates through the external boundary layer film of liquid surrounding the outside of the particle, followed by solute movement from the particles surface into internal sites by pore and/or surface diffusion and finally the adsorbate is adsorbed onto active sites at the interior of the adsorbent particles [18]. The final step is assumed to be rapid with respect to the first two steps and is, thus, not considered in kinetic analysis.

From the plots of q_t versus $t^{0.5}$ for various dyes, multilinearities are observed in Fig. 2, implying that more than one process affect the adsorption. The first portion of the plots, attributed to

Table 2
Parameters of kinetic model of MO, OIV, AF and X-3B adsorption onto NH_3^+-MCM-41

C_0 ($mmol\,L^{-1}$)	Dye	Pseudo-first-order model			Pseudo-second-order model			Intraparticle diffusion			
		k_1 (min^{-1})	q_e ($mmol\,g^{-1}$)	Δq (%)	k_2 ($g\,mmol^{-1}\,min^{-1}$)	q_e ($mmol\,g^{-1}$)	Δq (%)	k_{1P} ($mmol\,g^{-1}\,min^{0.5}$)	k_{2P} ($mmol\,g^{-1}\,min^{0.5}$)	k_{3P} ($mmol\,g^{-1}\,min^{0.5}$)	Δq (%)
0.21	MO	0.148	0.86	15.00	232	0.93	7.55	0.246	0.0876	0.0104	2.58
0.3		0.188	0.90	15.41	293	0.97	8.69	0.319	0.0771	0.0149	2.86
0.42		0.213	0.90	14.50	343	0.96	7.94	0.334	0.0720	0.0131	3.00
0.21	OIV	0.063	0.71	26.14	107	0.78	18.17	0.148	0.0651	0.0188	3.18
0.3		0.047	0.80	28.30	83	0.85	20.63	0.182	0.0562	0.0157	3.11
0.42		0.052	0.81	28.23	96	0.86	21.18	0.223	0.0622	0.0141	1.92
0.15	AF	0.096	0.29	16.92	452	0.31	8.69	0.0622	0.0337	0.0053	2.73
0.2		0.138	0.29	16.76	710	0.31	11.10	0.0933	0.0371	0.0022	6.10
0.3		0.240	0.29	18.87	1126	0.31	13.07	0.125	0.0193	0.0073	2.96
0.06	X-3B	0.018	0.24	44.04	94	0.27	36.72	0.0491	0.011	–	3.16
0.09		0.048	0.18	36.60	374	0.19	29.69	0.0527	0.0075	–	2.67
0.15		0.020	0.21	43.31	126	0.24	36.72	0.0554	0.0096	–	4.74

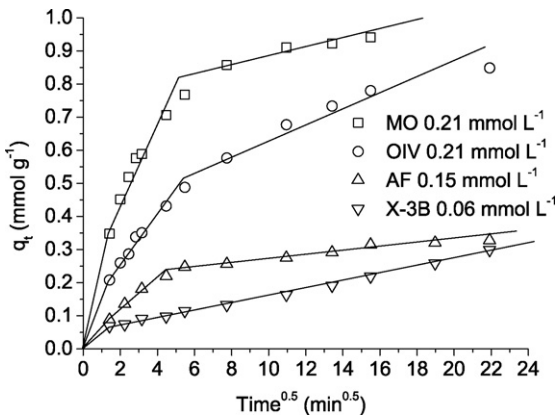

Fig. 2. Plot of q_t vs. $t^{0.5}$ at different dyes.

the diffusion of anionic dyes from the solution to the exterior surface of adsorbent, and which starts at onset of the process, is the fastest. When the adsorption of the exterior surface reaches saturation, the molecular dye enters into the pores of NH_3^+-MCM-41 particles and is adsorbed by the interior surface of the particles. The second portion of plots seems to refer to the diffusion into wider mesopores and the third portion with the lowest slope refers to adsorption into narrow mesopores. Similar kinetic results have also been reported in literatures [19,20]. If the intraparticle diffusion is the only rate-controlling step, the plot passes through the origin. If not, the boundary layer diffusion controls the adsorption to some degrees. It could be deduced from Fig. 2 that there are three processes that control the rate of dye adsorption, but only one process is rate limiting in any particular time range. Additionally, the lower slope corresponds to a slower adsorption process. This implies that the intraparticle diffusion of dye molecules into small mesopores is the rate-limiting step in the adsorption process on NH_3^+-MCM-41. Moreover, the slope of the second portion of the plots follows the order of MO > OIV > AF > X-3B which might arise from the difference in the dye molecule size.

3.2. Adsorption isotherm

The adsorption isotherms at 24.5 ± 0.5 °C, pH 5.6 of the four selected anionic dyes on the NH_3^+-MCM-41 with a solid/liquid ratio of 0.5 g L^{-1} are presented in Fig. 3. The shape of the isotherms looks rectangular because at low equilibrium dye concentration C_e, the equilibrium adsorption capacity q_e of the NH_3^+-MCM-41 reaches almost the same q_e as those at high equilibrium dye concentrations, showing that the adsorption process is independent of the initial dye concentration. It indicates that a strong affinity takes place between the dye molecules and the polar surface sites on NH_3^+-MCM-41. The rectangular shape of the isotherms was also obtained by other researchers [21,22]. The amount of adsorption is around 1.1, 1.1, 0.43, and 0.34 mmol g^{-1} for MO, OIV, AF and X-3B, respectively.

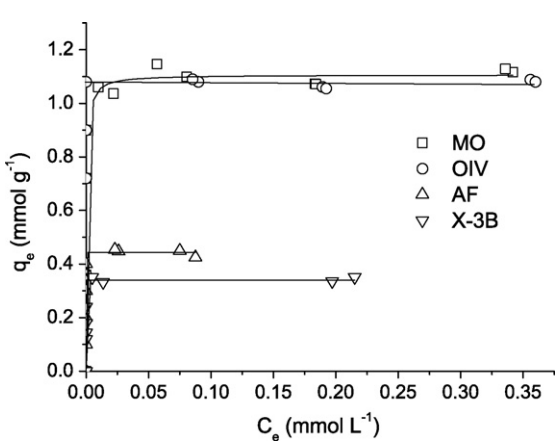

Fig. 3. Adsorption isotherm of dyes on NH_3^+-MCM-41.

Table 3
Langmuir isotherm constants for four anionic dyes adsorption onto NH_3^+-MCM-41

Dye	Langmuir model	
	Q_0 (mmol g^{-1})	R^2
MO	1.12	0.999
OIV	1.09	1.000
AF	0.43	0.997
X-3B	0.34	0.999

As also seen in Fig. 3, the adsorption of four types of anionic dyes onto NH_3^+-MCM-41 forms a typical Langmuir-type isotherm. Therefore, the obtained experimental equilibrium adsorption data are then fitted using Langmuir model (Eq. (8)).

$$q_e = \frac{Q_0 K_L C_e}{1 + K_L C_e} \tag{8}$$

where q_e (mmol g^{-1}) is the adsorbed amount of dye; C_e (mmol L^{-1}) is the equilibrium concentration of dye in solution; Q_0 (mmol g^{-1}) is the maximum monolayer adsorption capacity; K_L (L $mmol^{-1}$) is the constant related to the free energy of adsorption. A plot of C_e/q_e versus C_e gives a straight line of slope $1/Q_0$ and intercept $1/Q_0K_L$, where Q_0 gives the theoretical monolayer saturation capacity. Therefore, a linear expression for the Langmuir equation is:

$$\frac{C_e}{q_e} = \frac{1}{Q_0 K_L} + \frac{C_e}{Q_0} \tag{9}$$

The adsorption data were analyzed using the linear form (Eq. (9)) of the Langmuir isotherm. The corresponding parameters are shown in Table 3. It is clear that the fits are quite well for all the four anionic dyes under the concentration range studied (correlation coefficient, $R^2 > 0.997$), suggesting that the adsorption of four anionic dyes onto NH_3^+-MCM-41 closely follow a Langmuir isotherm. The high fit to the Langmuir model for the four anionic dyes also suggests that the adsorption is limited with monolayer coverage and the surface is relatively homogeneous. On the other hand, the maximum monolayer adsorption capacity (Q_0) varies in the order MO > OIV > AF > X-3B. The adsorption capacity of the MO is significantly higher than that of the X-3B, as manifested by the approximately 3.3-fold higher adsorption capacity of the MO. This may be due to the different molecular sizes and anionic groups of the two dyes. The larger dye molecule offers major resistance to penetration into the adsorbent mesoporous structure due to the pore blockage [10]. As NH_3^+-MCM-41 particles exhibit positive charge in water, electrostatic interaction will favor the adsorption of anionic dyes on NH_3^+-MCM-41. Hence, more anionic groups of dye adsorbed on NH_3^+-MCM-41 surfaces will decrease the adsorbent surface electrostatic field, and finally, decrease the dye adsorption.

The Langmuir isotherm constant related to the free energy of adsorption (k_L) could not be established because the intercepts of plots of C_e/q_e versus C_e are negative. Table 4 lists the comparison of maximum monolayer adsorption capacity of anionic dyes on various adsorbents. Compared with some data in literature, Table 4 shows that the NH_3^+-MCM-41 studied in this work have relatively high adsorption capacity of four anionic dyes at 24.5 ± 0.5 °C, pH 5.6.

Table 4
Comparison of the maximum monolayer adsorption capacities of four anionic dyes on various adsorbents

Dye	Adsorbent	Maximum monolayer adsorption capacities (mmol g^{-1})	Reference
MO	NH_3^+-MCM-41	1.12	This work
	Banana peel	0.064	[23]
	Orange peel	0.063	[23]
	Activated Carbon	0.029	[24]
	Modified sporopollenin	0.016	[25]
OIV	NH_3^+-MCM-41	1.09	This work
AF	NH_3^+-MCM-41	0.43	This work
X-3B	NH_3^+-MCM-41	0.34	This work
	Organic aerogels	0.14	[26]
	Carbon aerogels	0.92	[26]

3.3. Effect of pH and competitive anions on dye adsorption

The pH of solution is one of the most important parameters affecting the adsorption process. In order to determine the effect of pH on the adsorption capacity of NH_3^+-MCM-41, solutions were prepared at different pH values ranging from 4.0 to 11.0. The dependence of pH on the adsorption of four anionic dyes onto NH_3^+-MCM-41 is illustrated in Fig. 4. It is evident that the adsorption behavior of each anionic dye is similar from pH 4.0 to pH 10.0. For MO, OIV and X-3B, the adsorption capacities of the anionic dyes are affected slightly by the pH ranging from 4.0 to 8.0 and the average adsorption capacity is 0.87, 0.85 and 0.24 mmol g^{-1}, respectively. For AF, the adsorption capacity remains almost constant up to pH 7.0 and the average adsorption capacity is 0.41 mmol g^{-1}. However, a large decrease in adsorption capacity for all anionic dyes is observed under basic conditions. The adsorption capacity decreases from 0.88, 0.83, 0.23 and 0.37 mmol g^{-1} at around pH 8.0 to 0.22, 0.47, 0.18 and 0.04 mmol g^{-1} at around pH 10.0 for MO, OIV, X-3B and AF, respectively. This can be attributed to the electrostatic attraction between the negatively charged dye and the positively charged surface of NH_3^+-MCM-41. The increase in solution pH increases the number of hydroxyl groups, thus, decreases the number of positively charged sites and reduces the attraction between dye and adsorbent surface. Thus, as pH is increased, the surface functional group, NH_3^+, deprotonates and recovers their free amine form, which results in a decrease in surface charge density and is unable to exert any electrostatic effect toward anionic species [13]. On the other hand, the obvious decrease in the adsorption capacity of anionic dyes at high pH may be due to the decrease in the structure stability of NH_3^+-MCM-41 (such as the dissolution of NH_3^+-MCM-41 in basic solution) [9]. This implies that the adsorption of anionic dye onto NH_3^+-MCM-41could be enhanced at pH range 4.0–8.0.

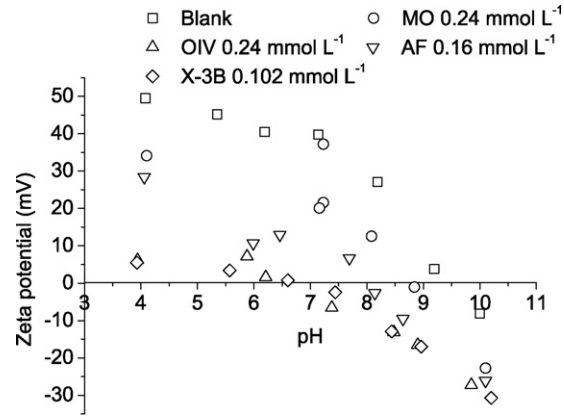

Fig. 5. The zeta potential of NH_3^+-MCM-41 as a function of pH at 24.5 ± 0.5 °C in the absence and presence of four anionic dyes using 0.01 mol L^{-1} NaCl as the supporting electrolyte.

Zeta potential can be an excellent tool to describe the interaction at solid/solution interfaces. Zeta potentials of NH_3^+-MCM-41 and NH_3^+-MCM-41 in equilibrium with MO, OIV, AF and X-3B in single aqueous solutions were investigated and the results are shown in Fig. 5. The isoelectric point (iep) of NH_3^+-MCM-41 is observed at pH 9.5. Below this pH, NH_3^+-MCM-41 particles are positive and above it they are negative. The iep values of NH_3^+-MCM-41 in the presence of MO, OIV, AF and X-3B were found to shift toward lower values. Under the experimental conditions, all dyes are negatively charged and the adsorption of these species leads to a negative charge. Moreover, although the zeta potential changes obviously at pHs range 4.0–8.0, the variation of zeta potential of NH_3^+-MCM-41 at different pHs is slight from an overall view point and the effects of pHs on the adsorption capacity of anionic dyes are small. From the above analysis, it is evident that electrostatic interaction was the main mechanism for the dye adsorption. The adsorption process can be described by the following reaction:

$$-NH_3^+ + Dye^- \rightarrow -NH_3^+ \cdots Dye^- \quad (10)$$

where $-NH_3^+$ represents the positive site and Dye^- represents the dye ion.

Anion is common in the hydrosphere, such as phosphate, nitrate, sulfate and carbonate. The effect of these anions on dye adsorption by NH_3^+-MCM-41 is shown in Fig. 6. It is observed that the

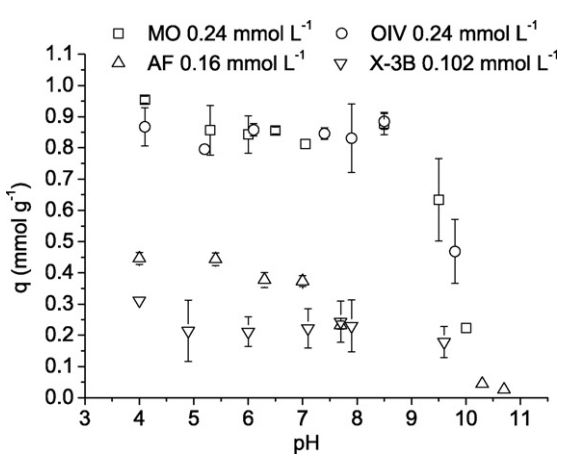

Fig. 4. Effect of solution pH on dye adsorption by NH_3^+-MCM-41.

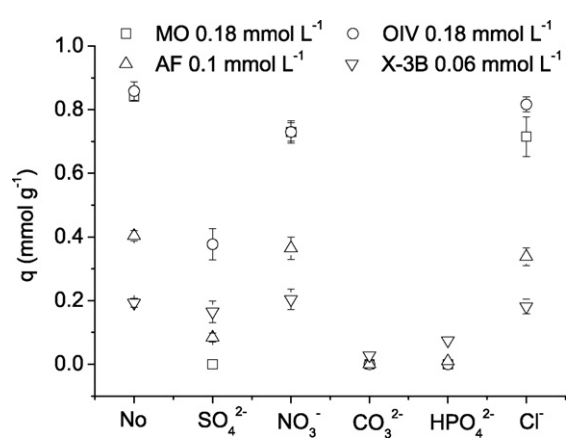

Fig. 6. Effect of competitive anion on dye adsorption by NH_3^+-MCM-41.

adsorption capacity of four anionic dyes is suppressed by less than 15% in the presence of nitrate and chloride anions. However, the presence of CO_3^{2-} and HPO_4^{2-} causes a large suppression of the adsorption capacity of all anionic dyes. In the presence of SO_4^{2-}, the adsorption capacity of X-3B remains constant; the adsorption capacity of OIV is 0.38 mmol g^{-1} which is 43.9% of the adsorption capacity in the absence of the anion. However, the adsorption of MO and AF is significantly inhibited by SO_4^{2-}. The degree of inhibition of all anions on the adsorption follows the order of $CO_3^{2-} \approx HPO_4^{2-} > SO_4^{2-} > NO_3^- \approx Cl^-$. It is noted that the anion of very soft acid has stronger inhibition impact for the adsorption capacity. Therefore, it is assumed that the high selectivity to the target dyes would be attributed to the specific interaction between the surface functional group NH_3^+ and the competitive anion.

4. Conclusions

The present study shows that ammonium-functionalized MCM-41 has a high affinity to four types of anionic dyes, MO, OIV, X-3B and AF. The amount of dye uptake was found to increase with the increase of contact time. The equilibrium time was independent of initial dye concentration. The adsorption kinetic studies showed that the adsorption process followed intraparticle diffusion model and more than one process affected the adsorption. The removal rate was dependent on both external mass transfer and intraparticle diffusion. The low values of the intraparticle diffusion rate constant indicated the significant influence of intraparticle diffusion on the kinetic control. Langmuir model was successfully applied to show that the adsorption was localized to a monolayer. Furthermore, the adsorption capacity followed the order of MO > OIV > AF > X-3B. The maximum adsorption amounts were 1.12, 1.09, 0.43 and 0.34 mmol g^{-1} for MO, OIV, AF and X-3B, respectively. At pH range from 4.0 to 8.0, the adsorption capacity of dye was slightly changed by pH. However, at pH above 8.0, the adsorption capacity of dye decreased significantly due to the increasing number of hydroxyl groups and the unstable structure of NH_3^+-MCM-41. In the presence of competitive anions, dye uptake was notably inhibited by the anion of very soft acid such as CO_3^{2-} and HPO_4^{2-}. The zeta potential of NH_3^+-MCM-41 decreased after dye was adsorbed, showing that the electrostatic interaction was considered as the main mechanism for the dye adsorption.

Acknowledgment

The authors are grateful for the financial support provided by the Ministry of Education of China (Project 705013).

References

[1] P.C.C. Faria, J.J.M. Órfão, M.F.R. Pereira, Adsorption of anionic and cationic dyes on activated carbons with different surface chemistries, Water Res. 38 (2004) 2043–2052.
[2] F.P. van der Zee, S. Villaverde, Combined anaerobic-aerobic treatment of azo dyes—a short review of bioreactor studies, Water Res. 39 (2005) 1425–1440.
[3] G. Crini, Non-conventional low-cost adsorbents for dye removal: a review, Bioresour. Technol. 97 (2006) 1061–1085.
[4] E.N. El Qada, S.J. Allen, G.M. Walker, Adsorption of methylene blue onto activated carbon produced from steam activated bituminous coal: a study of equilibrium adsorption isotherm, Chem. Eng. J. 124 (2006) 103–110.
[5] E. Forgacs, T. Cserháti, G. Oros, Removal of synthetic dyes from wastewaters: a review, Environ. Int. 30 (2004) 953–971.
[6] P.V. Messina, P.C. Schulz, Adsorption of reactive dyes on titania-silica mesoporous materials, J. Colloid Interface Sci. 299 (2006) 305–320.
[7] S. Wang, Z.H. Zhu, Characterisation and environmental application of an Australian natural zeolite for basic dye removal from aqueous solution, J. Hazard. Mater. B136 (2006) 946–952.
[8] X.S. Zhao, G.Q. Lu, G.J. Millar, Advances in mesoporous molecular sieve MCM-41, Ind. Eng. Chem. Res. 35 (1996) 2075–2090.
[9] P. Selvam, S.K. Bhatia, C.G. Sonwane, Recent Advances in processing and characterization of periodic mesoporous MCM-41 silicate molecular sieves, Ind. Eng. Chem. Res. 40 (2001) 3237–3261.
[10] L. Juang, C. Wang, C. Lee, Adsorption of basic dyes onto MCM-41, Chemosphere 64 (2006) 1920–1928.
[11] S. Wang, H. Li, L. Xu, Application of zeolite MCM-22 for basic dye removal from wastewater, J. Colloid Interface Sci. 295 (2006) 71–78.
[12] C. Lee, S. Liu, L. Juang, C. Wang, K. Lin, M. Lyu, Application of MCM-41 for dyes removal from wastewater, J. Hazard. Mater. 147 (2007) 997–1005.
[13] R. Saad, K. Belkacemi, S. Hamoudi, Adsorption of phosphate and nitrate anions on ammonium-functionalized MCM-48: effects of experimental conditions, J. Colloid Interface Sci. 311 (2007) 375–381.
[14] T. Yokoi, T. Tatsumi, H. Yoshitake, Fe^{3+} coordinated to amino-functionalized MCM-41: an adsorbent for the toxic oxyanions with high capacity, resistibility to inhibiting anions, and reusability after a simple treatment, J. Colloid Interface Sci. 274 (2004) 451–457.
[15] M. Broyer, S. Valange, J.P. Bellat, O. Bertrand, G. Weber, Z. Gabelica, Influence of aging, thermal, hydrothermal, and mechanical treatments on the porosity of MCM-41 mesoporous silica, Langmuir 18 (2002) 5083–5091.
[16] A. Walcarius, M. Etienne, J. Bessière, Rate of access to the binding sites in organically modified silicates. 1. Amorphous silica gels grafted with amine or thiol groups, Chem. Mater. 14 (2002) 2757–2766.
[17] Y.S. Ho, J.C.Y. Ng, G. McKay, Kinetics of pollutant sorption by biosorbents: review, Separ. Purif. Meth. 29 (2000) 189–232.
[18] S.D. Faust, O.M. Aly, Adsorption Processes for Water Treatment, Butterworth Publishers, Massachusetts, 1987.
[19] E. Lorenc-Grabowska, G. Gryglewicz, Adsorption of lignite-derived humic acids on coal-based mesoporous activated carbons, J. Colloid Interface Sci. 284 (2005) 416–423.
[20] M. Basibuyuk, C.F. Forster, An examination of the adsorption characteristics of a basic dye (Maxilon Red BL-N) on to live activated sludge system, Process Biochem. 38 (2003) 1311–1316.
[21] M. Chiou, H. Li, Equilibrium and kinetic modeling of adsorption of reactive dye on cross-linked chitosan beads, J. Hazard. Mater. B93 (2002) 233–248.
[22] A. Gücek, S. Şener, S. Bilgen, M. Ali Mazmancı, Adsorption and kinetic studies of cationic and anionic dyes on pyrophyllite from aqueous solutions, J. Colloid Interface Sci. 286 (2005) 53–60.
[23] G. Annadurai, R. Juang, D. Lee, Use of cellulose-based wastes for adsorption of dyes from aqueous solutions, J. Hazard. Mater. B92 (2002) 263–274.
[24] K.P. Singh, D. Mohan, S. Sinha, G.S. Tondon, D. Gosh, Color removal from wastewater using low-cost activated carbon derived from agricultural waste material, Ind. Eng. Chem. Res. 42 (2003) 1965–1976.
[25] A. Ayar, O. Gezici, M. Küçükosmanoğlu, Adsorptive removal of methylene blue and methyl orange from aqueous media by carboxylated diaminoethane sporopollenin: on the usability of an aminocarboxilic acid functionality-bearing solid-stationary phase in column techniques, J. Hazard. Mater. 146 (2007) 186–193.
[26] X. Wu, D. Wu, R. Fu, Studies on the adsorption of reactive brilliant red X-3B dye on organic and carbon aerogels, J. Hazard. Mater. 147 (2007) 1028–1036.